Research Square

Preprints are preliminary reports that have not undergone peer review.
They should not be considered conclusive, used to inform clinical practice,
or referenced by the media as validated information.

Advancing translational readthrough therapies: genetic and mechanistic insights in Choroideremia nonsense mutation models

Laura Lentini

laura.lentini@unipa.it

University of Palermo Dip. STEBICEF https://orcid.org/0000-0002-1355-8252

Emanuele Vitale

University of Palermo Dip. STEBICEF

Raffaella Melfi

University of Palermo Dip. STEBICEF

Saleem Bhat

University of Pennsylvania (UPENN)

Ignazio Fiduccia

University of Palermo Dip. STEBICEF

Sefora Marino

University of Palermo Dip. STEBICEF

Davide Ricci

University of Palermo Dip. STEBICEF

Riccardo Varrica

University of Palermo Dip. STEBICEF

Maria Grazia Zizzo

University of Palermo Dip. STEBICEF

Carla Rizzo

University of Palermo Dip. STEBICEF

Ivana Pibiri

University of Palermo Dip. STEBICEF

Andrea Pace

Università degli Studi di Palermo

Barry Cooperman

University of Pennsylvania

Article

Keywords:

Posted Date: March 5th, 2026

DOI: https://doi.org/10.21203/rs.3.rs-9030140/v1

License: This work is licensed under a Creative Commons Attribution 4.0 International License.
Read Full License

Additional Declarations: There is **NO** Competing Interest.

Advancing translational readthrough therapies: genetic and mechanistic insights in Choroideremia nonsense mutation models

Emanuele Vitale[1], Raffaella Melfi[1], Saleem Bhat[2], Ignazio Fiduccia[1], Sefora Marino1, Davide Ricci[1], Riccardo Varrica[1], Maria Grazia Zizzo[1], Carla Rizzo[1], Ivana Pibiri[1,*], Andrea Pace[1], Barry S. Cooperman[2] and Laura Lentini[1,*]

[1]Department of Biological, Chemical and Pharmaceutical Sciences and Technologies, University of Palermo, Palermo, Italy.

[2]Department of Chemistry, University of Pennsylvania, Philadelphia, USA.

[*]Corresponding authors: laura.lentini@unipa.it ;ivana.pibiri@unipa.it

Abstract

Nonsense variants account for approximately 11% of rare genetic diseases and represent a severe class of mutations for which effective therapies are still lacking. One promising strategy is suppression therapy using translational readthrough-inducing drugs (TRIDs). In this study, we investigated the mechanisms of action and readthrough activity of three TRIDs, NV848, NV914, and NV930, in models of Choroideremia, an X-linked retinal degenerative disease caused by nonsense mutations in the *CHM* gene. Using the PURE-LITE cell-free translation system, we assessed their ability to promote readthrough and interfere with release factor–mediated termination, revealing mechanisms distinct from that of PTC124. To evaluate their therapeutic potential in cellular contexts, we developed two engineered Choroideremia nonsense cell models and analyzed REP1 protein rescue in patient-derived primary fibroblasts. All three compounds effectively induced readthrough both in the cell-free system and in cellular models, supporting their potential as candidates for treating nonsense mutation-associated retinal diseases.

Introduction

Nonsense variants are a major cause of severe monogenic diseases and are estimated to account for approximately 10–11% of genetic disorders worldwide. These variants typically arise from single-nucleotide substitutions that introduce premature termination codons (PTCs) into mRNA coding sequences [**1**]. PTCs interrupt normal translation, leading to truncated and nonfunctional proteins that are frequently degraded by intracellular quality-control pathways, such as nonsense-mediated mRNA decay (NMD) or proteasome-dependent degradation [**2**]. The absence or dysfunction of these proteins underlies a wide range of genetic diseases, including Choroideremia (CHM), Cystic Fibrosis (CF), Duchenne Muscular Dystrophy (DMD), Shwachman-Diamond syndrome, and several forms of cancer [**1**-**2**]. In the last few decades, personalised medicine has gained prominence as an approach that tailors therapies to individual genetic, physiological, environmental, and behavioural factors. Advances in DNA sequencing, proteomics, and imaging now allow precise patient stratification,

suggesting new therapeutic strategies for nonsense diseases [**3**]. Among the various approaches explored, such as gene and RNA editing, NMD inhibition, and anticodon-engineered tRNAs, the nonsense suppression therapy has emerged as particularly promising [**4**]. This strategy relies on translational readthrough-inducing drugs (TRIDs) molecules that promote the insertion of near-cognate tRNAs at PTCs, thereby allowing the synthesis of full-length, functional proteins [**5**]. Aminoglycosides such as gentamicin, tobramycin, and paromomycin were among the first molecules identified to induce readthrough, acting by impairing ribosomal proofreading. Although these compounds showed significant readthrough activity, their clinical application has been severely limited by renal, auditory, and vestibular toxicities [**6-8**]. To overcome these limitations, alternative TRIDs have been developed. Among them, PTC124 (also known as Ataluren) has been shown to promote PTC readthrough, particularly at UGA codons, without the toxic effects associated with aminoglycosides. Clinical trials demonstrated therapeutic benefit in subsets of patients with nonsense-mutation DMD, leading to its conditional approval under the trade name Translarna [**9-12**]. However, PTC124 has not shown significant rescue of REP1 activity in CHM cellular models harbouring UAA nonsense variants, leaving CHM, a rare X-linked retinal dystrophy in which 34% of cases are linked to nonsense mutations, without treatment [**5**]. The need for novel, effective, and low-toxicity TRIDs remains urgent, particularly for rare or "orphan" diseases. In this context, our research group has recently developed three patented PTC124-derived compounds, TRIDs: NV848, NV914, and NV930 (**Figure 1**), which display high readthrough activity with no detectable toxicity *in vitro* or *in vivo*, and do not induce off-target effects [**13-15**]. Despite their therapeutic promise, the biological targets and precise mechanisms of action of these NV compounds remain unknown. This knowledge gap is particularly notable given recent studies showing that PTC124 binds multiple sites within the translation machinery and promotes readthrough by competing with release-factor-dependent termination [**16**].

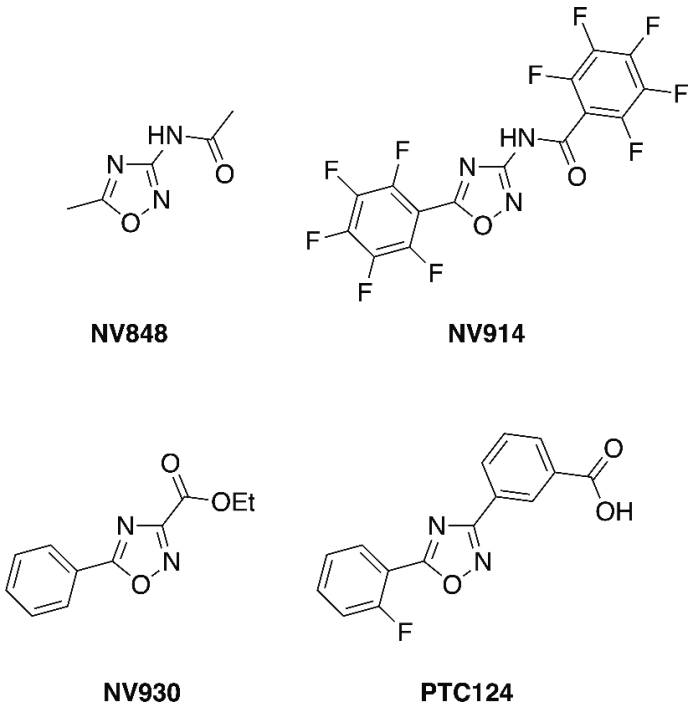


Figure 1. NV compounds and PTC124 structures.

To address this gap, the present study pursued two complementary objectives. First, we employed the highly purified eukaryotic cell-free PURE-LITE translation system to investigate the effects of NV compounds on ribosomal termination and readthrough at PTCs. This system utilises Cricket paralysis virus (CrPV) intergenic internal ribosome entry site (IRES) driven mRNAs to program 80S ribosomes and initiate translation in the absence of canonical initiation factors. PURE-LITE enables precise characterisation of the competition between eRF1/eRF3-mediated termination and readthrough mediated by near-cognate tRNAs in the presence of a PTC at the ribosomal A-site [**17,18**], using CrPV-IRES mRNAs containing either sense (UGG) or nonsense codon (UGA), which allow direct determination of the MoAs of the NV compounds in inducing readthrough. Second, we evaluated NV compound-induced protein rescue in two stable H1299 cell lines harbouring the most common CHM nonsense variants, R293X and R253X, as well as in patient-derived fibroblasts carrying the R253X, R270X, and S190X nonsense variants, to directly assess REP1 protein rescue.

RESULTS

PURE-LITE functional assays of cognate elongation, PTC readthrough, and termination.

We used the PURE-LITE system to determine the effects of NV compounds on rates of cognate elongation, PTC readthrough, and termination, as shown in **Figure 2**, using both co-sedimentation [**17,18**] and plate reader [**21,22**] assays.

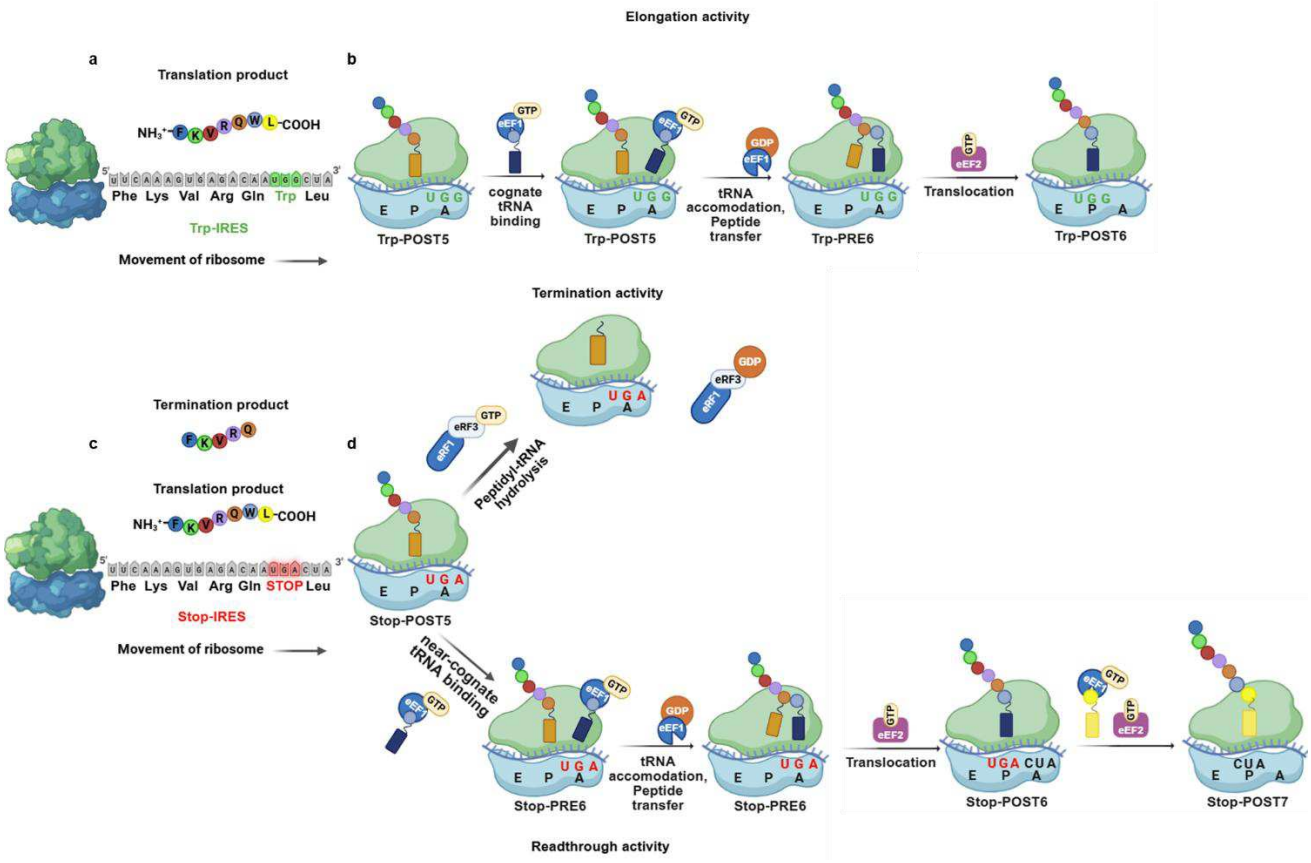


Figure 2. PURE-LITE elongation, readthrough, and termination schemes. a) *Trp-IRES encodes PheLysValArgGlnTrpLeu;* ***b)*** *Elongation reactions of Trp-POST5 complex;* ***c)****Stop-IRES encodes PheLysValArgGlnStopLeu;* ***d)*** *Termination and readthrough reactions of Stop-POST5 complex. Both Trp POST5 and Stop-POST5 complexes contain PheLysValArgGln-tRNA^{Gln} in the P-site; Adapted from Ng et al., 2021*

NV compounds had no significant effect either on cognate peptide elongation (**Figure 3-A**), as measured by Trp-POST5 conversion to Trp-POST6, on the addition of tryptophan ternary complex (Trp-TC, Trp-tRNA^{Trp}.eEF1A.GTP) and eEF2.GTP, or on termination, on addition of release factor complex (RFC, eRF1.eRF2.GTP) to the Stop-POST5 complex (**Figure 3-B**). In contrast, all three NV compounds markedly stimulate readthrough, with NV848 being the most potent (**Figure 3-C**), reaching its saturation value at a concentration at least a factor of ten lower than either NV914 or NV930 (**Figure S1**). Significantly, all three NV compounds have lower EC_{50} values for readthrough stimulation than we previously reported for PTC124 (~300 µM) [**18**].

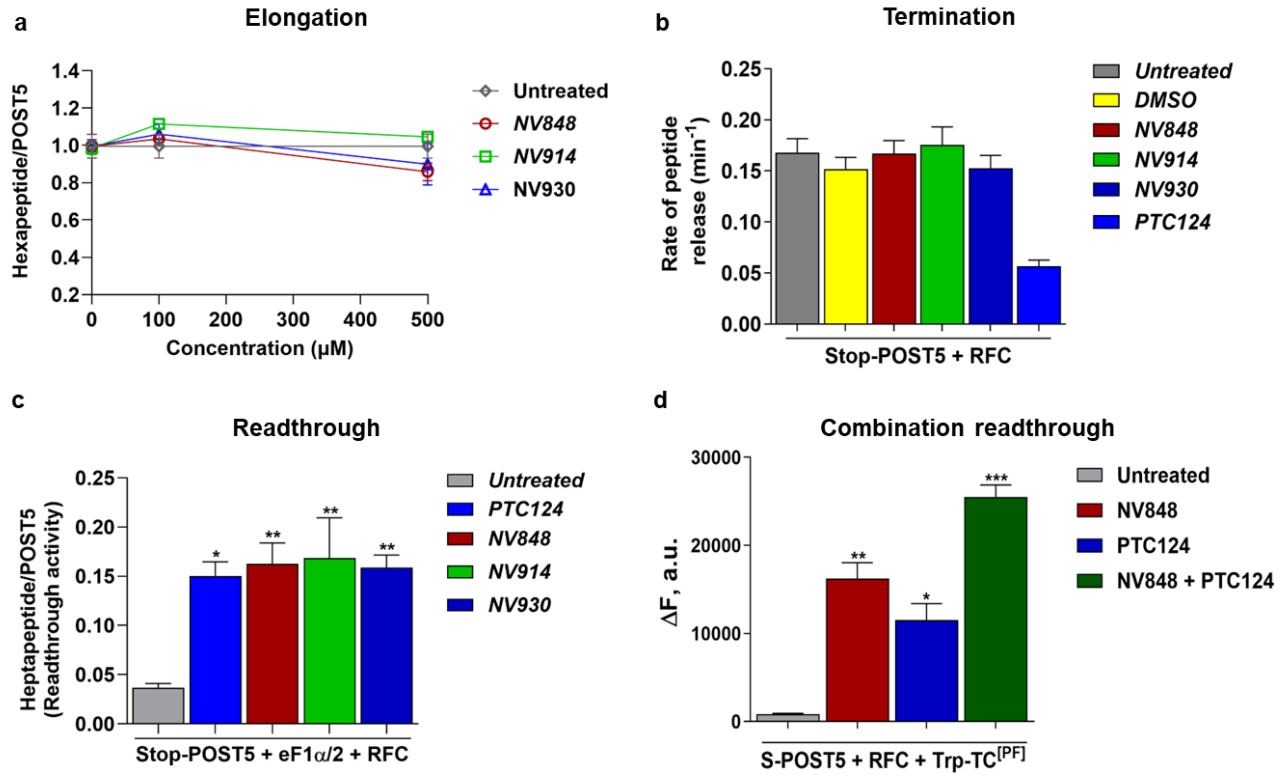


Figure 3. Assays of NVS compound activity. a) Elongation activity: *Lack of NV compound effect on elongation as measured by Trp-POST6 formation using a co-sedimentation assay in the presence of NV848, NV914, or NV930 at 100 μM and 500 μM. Reaction components were Trp-POST5 (0.05 μM), [^{3}H-Trp]-TC (0.25 μM), and eEF2 (1 μM);* ***b) Termination activity:*** *Effects of TRIDs (all 500 μM) on the rate of peptide release from Stop-POST5 (0.04 μM) catalysed by RFC (0.075 μM) using the plate reader assay. No statistically significant difference in the rate of peptide release is observed after treatment with NV molecules, in contrast to the previously demonstrated marked inhibition by PTC124 [**18**];* ***c) Readthrough activity:*** *Readthrough was measured by the heptapeptidyl-tRNA^{Leu} formation assay at different near saturation concentrations of TRIDs (**see Figure S1**), NV848 (12 μM), NV914 (100 μM), NV930 (100 μM) and PTC124 (1 mM), other concentrations: Stop-POST5 (0.05 μM), RFC (0.05 μM), Trp-TC (0.25 μM), [^{3}H-Leu]-TC (0.25 μM), eEF1α (1 μM), eEF2 (1 μM);* ***d) Combination readthrough activity:*** *Additive effects of NV848 (12 μM) and PTC124 (1 mM) on readthrough measured by the plate reader assay for Stop-PRE6 formation from Stop-POST5[**22**]. Other concentrations: Stop-POST5 (0.05 μM), RFC (0.05μM), prf-labelled Trp-TC (0.1 μM). 1 mM GTP was used in all experiments. Data for all experiments were analysed using GraphPad Prism 6, which provided a* probability value (p) of one symbol (*) for p< 0.05, two symbols (**) for p < 0.01, three symbols (***) for p<0.001.

These results show that although the *a priori* design of the NV compounds was based on mimicry of PTC124, in fact their mechanisms of action are orthogonal to that of PTC124, stimulating readthrough directly while having no effect on termination, or on ternary complex binding (**Figure 3-A**) whereas PTC124 inhibits termination (**Figure 3-B**) and only stimulates readthrough indirectly because of such inhibition. A consequence of this orthogonality is that, when combined, they can have an additive effect on readthrough, as demonstrated by the combination of NV848 and PTC124 (**Figure 3-D**).

Generation of stable CHM nonsense cell models for REP1 rescue analysis using NV molecules

To evaluate NV compound-mediated rescue of REP1 expression, we generated cellular models harbouring two of the most prevalent CHM nonsense variants, R253X (c.757C>T) and R293X (c.877C>T). These mutations were introduced into a CHM-tGFP fusion construct by site-directed mutagenesis, enabling direct visualisation of full-length REP1 expression through GFP fluorescence (**Figure S2A**). Both variants convert the native arginine codon (CGA) into a premature UGA stop codon. Successful introduction of the mutations was confirmed by Sanger sequencing **(Figure S2B-E).** Sequence analysis verified precise incorporation of each nonsense mutation without additional alterations. These validated constructs were subsequently used to establish stable cell lines for downstream readthrough and protein rescue analyses.

Establishment and validation of stable H1299 cell lines harbouring CHM nonsense variants

To generate cellular models suitable for evaluating NV-mediated readthrough, H1299 cells were transfected with the validated CHM^{R253X}-tGFP and CHM^{R293X}-tGFP constructs and selected with G418 (600 μg/mL) to establish stable populations. Twenty-four hours after transfection, robust tGFP fluorescence was detected in cells expressing the wild-type CHM^{WT}-tGFP construct. In contrast, no fluorescence was observed in cells transfected with either CHM^{R253X}-tGFP or CHM^{R293X}-tGFP **(Figure S3),** confirming that both nonsense mutations abolish full-length REP1-tGFP expression. Following selection, stable cell populations were molecularly characterised. Genomic PCR confirmed integration of the CHM–tGFP constructs in all transfected lines **(Figure 4-A).** Quantitative RT-PCR demonstrated comparable levels of CHM–tGFP mRNA expression across wild-type and nonsense variants **(Figure 4-B),** indicating that the introduced mutations do not substantially affect transcript abundance. In contrast, Western blot analysis revealed the expression of full-length REP1-tGFP fusion protein only in CHM^{WT}-tGFP cells, while CHM^{R253X}-tGFP and CHM^{R293X}-tGFP cells expressed only endogenous REP1 **(Figure 4-C).** Consistent with this finding, after the 15-day cell selection, tGFP fluorescence was detectable exclusively in the wild-type line **(Figure 4-D).** Collectively, these data demonstrate that the R253X and R293X variants effectively abolish REP1-tGFP protein production without significantly altering mRNA levels, establishing robust and validated cellular models for assessing translational readthrough and protein rescue.

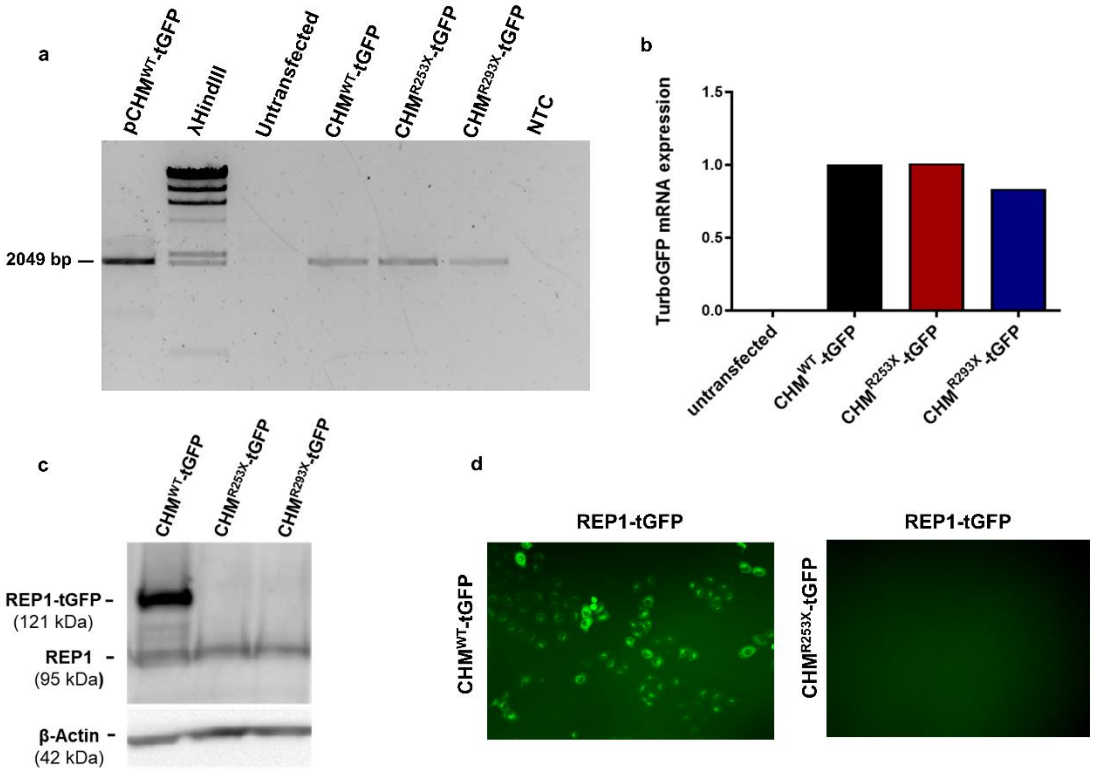


Figure 4. Production of stable H1299 CHM^{R253X}-tGFP and CHM^{R293X}-tGFP cell lines: ***a)*** *PCR analysis showing the integration of the mutagenized vector in the genomic DNA of H1299 cells. The pCHMWT-tGFP vector was used as a positive control; DNA from untransfected cells and a no-template control (NTC) were used as negative controls.* ***(b)*** *tGFP mRNA expression assessed by Real Time RT-PCR;* ***c)*** *Western blot analysis on H1299 cells transfected with pCHM^{WT}-tGFP, pCHM^{R253X}-tGFP, or pCHM^{R293X}-tGFP. The REP1 antibody was used to detect the REP1-tGFP protein (121 kDa) and the endogenous REP1 (95 kDa);* ***d)*** *Stable H1299 CHM^{WT}-tGFP cells showing*

Immunofluorescence analysis demonstrates NV-mediated REP1–tGFP rescue in CHM nonsense cell lines.

Having established stable H1299 cell lines harbouring the R253X and R293X nonsense variants, we next evaluated whether NV compounds restore REP1-tGFP expression in cells. Dose-response immunofluorescence analyses revealed that NV compounds induce robust rescue of REP1-tGFP in both CHM^{R253X}-tGFP **(Figure S4)** and CHM^{R293X}-tGFP **(Figure S5)** cell lines. Notably, NV848 achieved near-maximal rescue at 12 µM in both variants. Similarly, NV930 reached plateau levels at 12 µM in the R253X model, and NV914 did so in the R293X model. In contrast, PTC124 required higher concentrations to achieve comparable effects in both variants. NV914 in the R253X model and NV930 in the R293X model also displayed more gradual dose-response behavior.

This differential potency profile is consistent with the PURE-LITE readthrough data (**Figures 3 and S1**), in which NV848 exhibited the strongest activity. Based on these results, 12 µM was selected for subsequent rescue experiments. Following 72-hour treatment, all three NV compounds induced detectable REP1-tGFP expression in both R253X and R293X stable cell lines (**Figures 5 and 6**). Restored fluorescence was absent in untreated cells and comparable in pattern to that observed in wild-type controls, indicating successful translational readthrough and production of full-length fusion protein. Collectively, these data demonstrate that NV compounds effectively promote nonsense suppression in disease-relevant cellular models, with compound-specific differences in potency that mirror their biochemical activity in the reconstituted translation system.

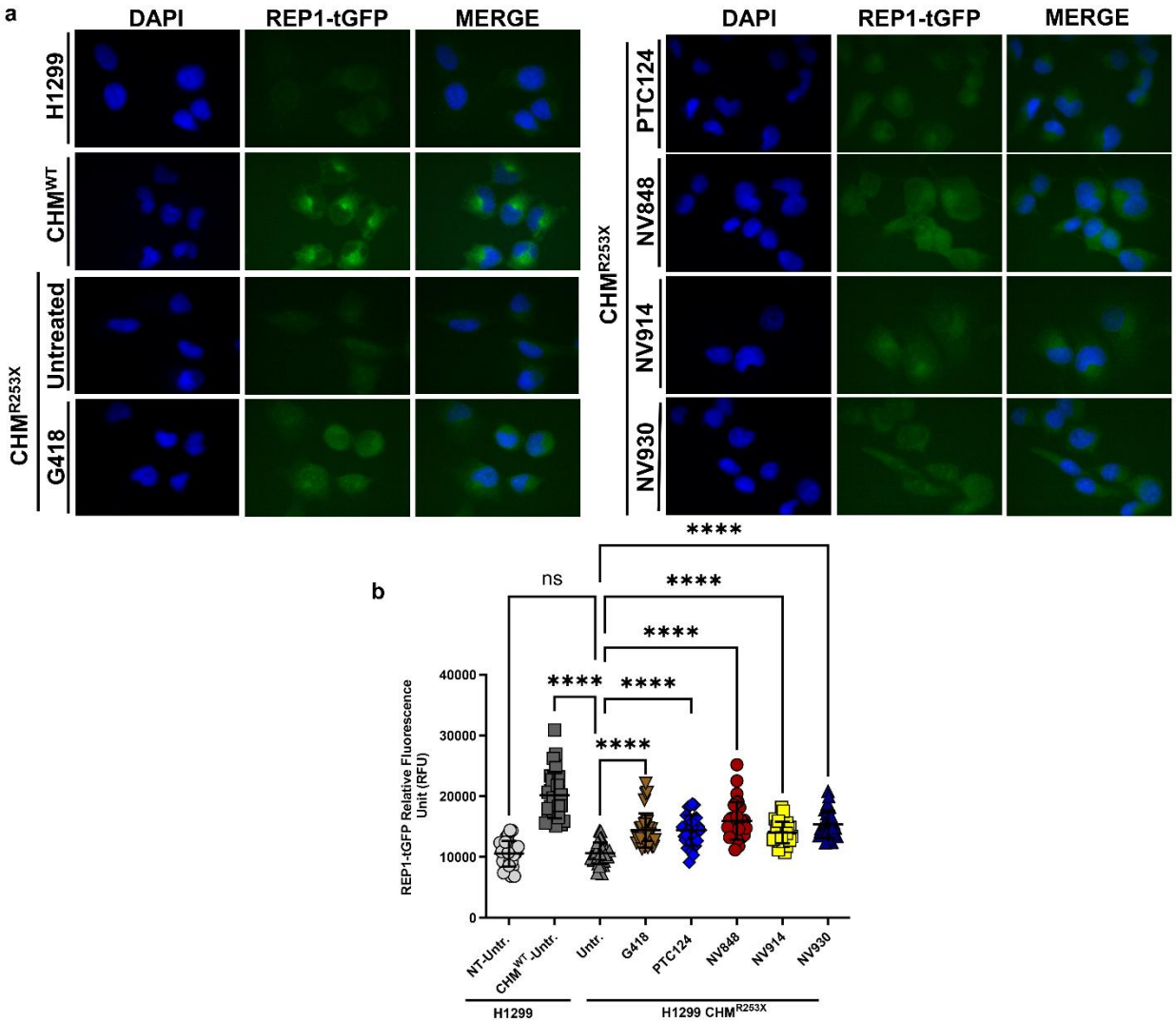


Figure 5. Panel showing immunofluorescence and quantification analyses: a) *Panels representative of immunofluorescence analyses performed on H1299 CHM^{R253X}-tGFP. H1299 not transfected (NT-Untr.) and H1299 CHM^{R253X}-tGFP untreated represent the negative control, while H1299 CHM^{WT}-tGFP represents the positive control;* ***b)*** *Quantification of immunofluorescence analyses performed on H1299 CHM^{R253X}-tGFP. All the images were collected by a Zeiss AxioSkope microscope at 63X. Data for all experiments were analysed using GraphPad Prism 6, which provided a* probability value (p) of four symbols (****) for $p < 0.0001$.

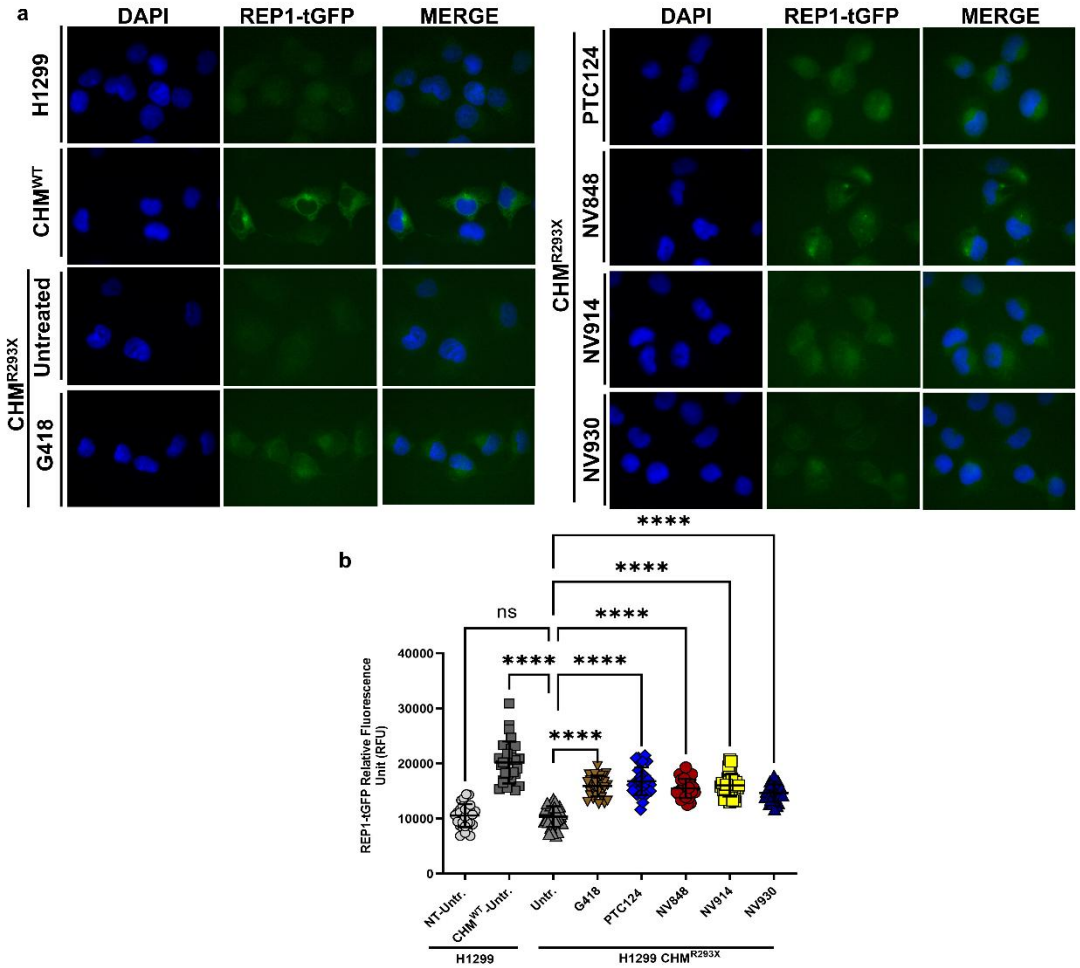


Figure 6. Panel showing immunofluorescence and quantification analyses: ***A)*** *Panels representative of immunofluorescence analyses performed on H1299 CHM^{R293X}-GFP. H1299 (NT-Untr.) and H1299 CHM^{R293X}-tGFP untreated represent the negative control, while H1299 CHM^{WT}-tGFP represents the positive control;* ***B)*** *Quantification of immunofluorescence analyses performed on H1299 CHM^{R293X}-tGFP. All images were acquired using a Zeiss AxioSkope microscope at 63X magnification. Data for all experiments were analysed using GraphPad Prism 6, which provided a* probability value (p) with four symbols (****) for $p < 0.0001$.

NV compounds do not substantially alter CHM transcript levels in patient-derived fibroblasts.

To determine whether NV-mediated REP1 rescue in primary cells results from translational readthrough rather than altered mRNA stability, we examined CHM transcript levels following chronic treatment in patient-derived fibroblasts carrying the R253X, S190X, or R270X nonsense variants. Quantitative RT-PCR analysis after 72 hours of treatment revealed that CHM mRNA levels remained largely unchanged across all conditions compared to untreated controls **(Figure S6A).** This was observed for all three NV compounds and for PTC124 as well. A modest but statistically significant increase in CHM transcript abundance was detected in R253X fibroblasts treated with NV914 **(Figure S6B),** whereas no consistent changes were observed in S190X or R270X cells. Overall, these results indicate that NV compounds do not broadly stabilize CHM transcripts or inhibit NMD in patient-derived fibroblasts. Therefore, any increase in REP1 protein levels observed upon

treatment is unlikely to arise from enhanced transcript accumulation, but rather from direct stimulation of translational readthrough at premature termination codons. Collectively, these findings support a mechanism in which NV compounds primarily act at the translational level rather than through mRNA surveillance.

NV compounds restore REP1 expression and reduce micronucleation in patient-derived fibroblasts.

To determine whether NV-mediated readthrough translates into functional protein restoration in a disease-relevant context, REP1 expression was evaluated in primary fibroblasts derived from male patients carrying the R253X, S190X, or R270X nonsense variants in *CHM*.

Immunofluorescence analyses revealed robust induction of REP1 protein following 72-hour treatment with NV848, NV914, or NV930 in all three patient-derived cell lines (**Figures 7-9**). In untreated fibroblasts, the REP1 signal was minimal or undetectable, consistent with loss of full-length protein due to premature termination. Upon NV treatment, REP1 staining became clearly detectable and comparable in distribution to that observed in positive control cells. Importantly, rescue was observed across distinct nonsense variants, indicating that NV activity is not restricted to a single sequence context. The magnitude of rescue was similar to that achieved with PTC124 under identical conditions.

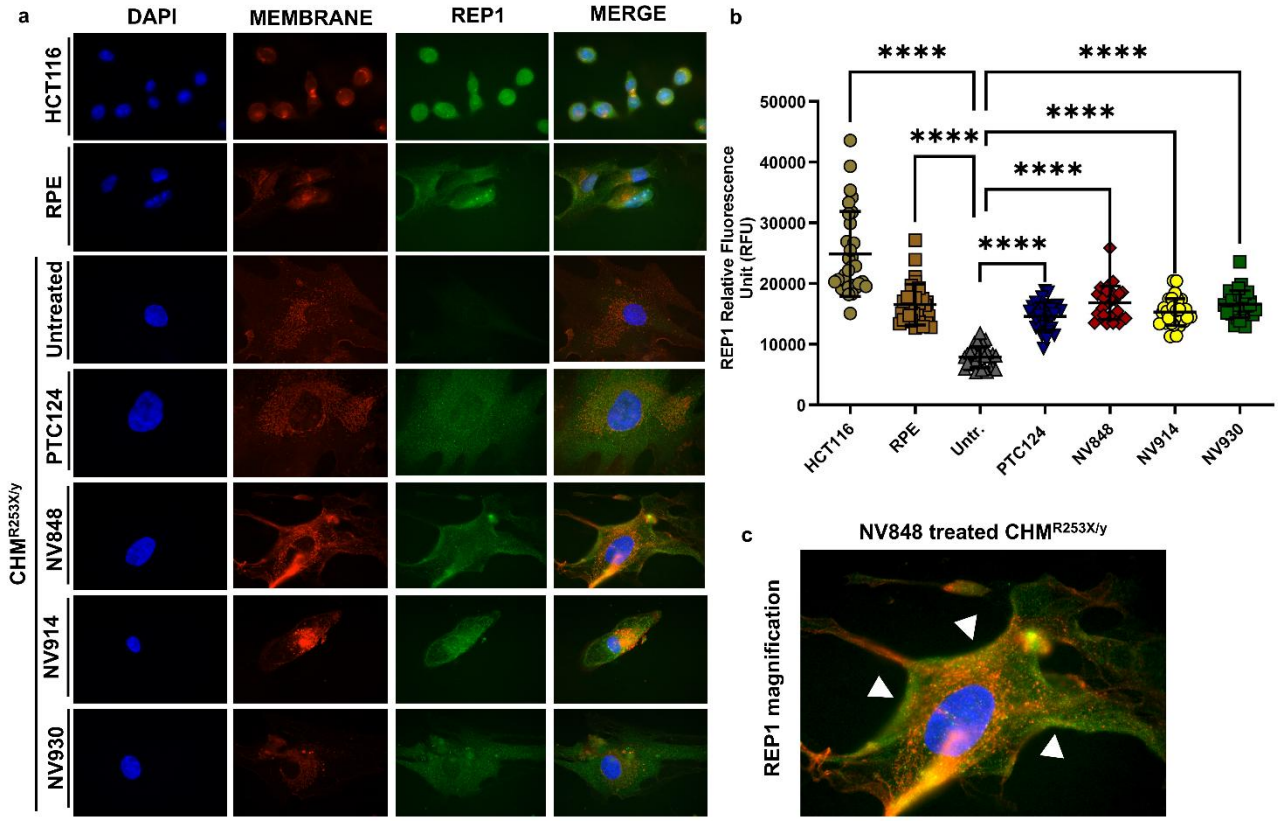


Figure 7. Immunofluorescence analyses on R253X patient-derived fibroblasts, showing the rescue of REP1 protein after 72hours at 12 µM NV molecules treatment: ***A****) REP1 protein (green) was revealed by a specific primary antibody and a fluorochrome-conjugated secondary antibody (AlexaFluor-488). Nuclei (blue) were stained with DAPI (40,6-diamidino-2-phenylindole). PTC124 was used as a positive control for PTCs readthrough.* ***B****) Images were quantified using ImageJ, and the quantifications were analyzed using GraphPad Prism 6 software, which provided* a probability value (p) of four symbols (****) for $p < 0.0001$*;* ***C****) REP1 magnification image of NV848 treated* $CHM^{R253X/y}$*, the arrowhead is showing the correct expression rescue of REP1 protein (green) inside the cells.*

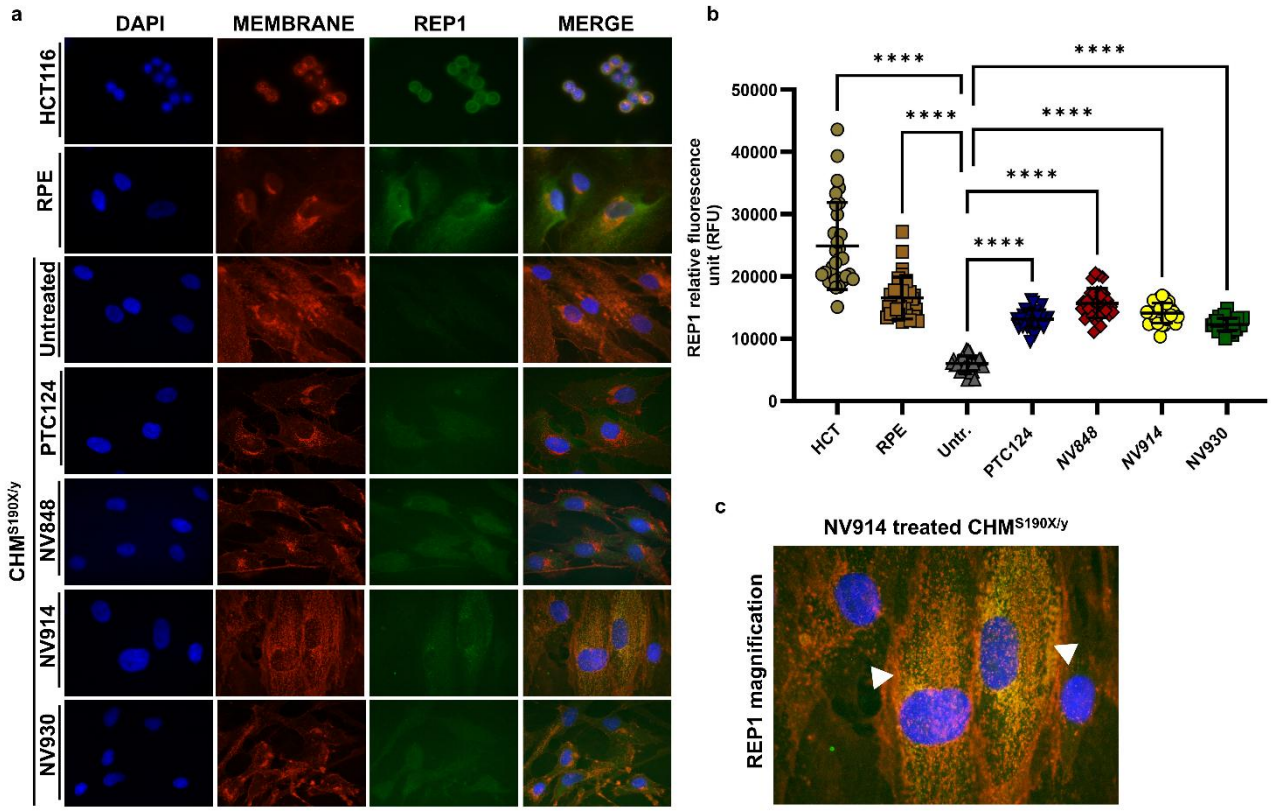


Figure 8. Immunofluorescence analyses on S190X patient-derived fibroblasts, showing the rescue of REP1 protein after 72hours of 12 µM NV molecules treatment: A) *REP1 protein (green) was revealed by a specific primary antibody and a fluorochrome-conjugated secondary antibody (AlexaFluor-488). Nuclei (blue) were stained with DAPI (40,6-diamidino-2-phenylindole). PTC124 was used as a positive control for PTCs readthrough.* ***B)*** *Images were quantified using ImageJ, and the quantifications were analyzed using GraphPad Prism 6 software, which provided* a probability value (p) of four symbols (****) for $p < 0.0001$*;* ***C)*** *REP1 magnification image of NV914 treated* $CHM^{S190X/y,}$ *the arrowhead shows the correct expression rescue of REP1 protein (green) inside the cells.*

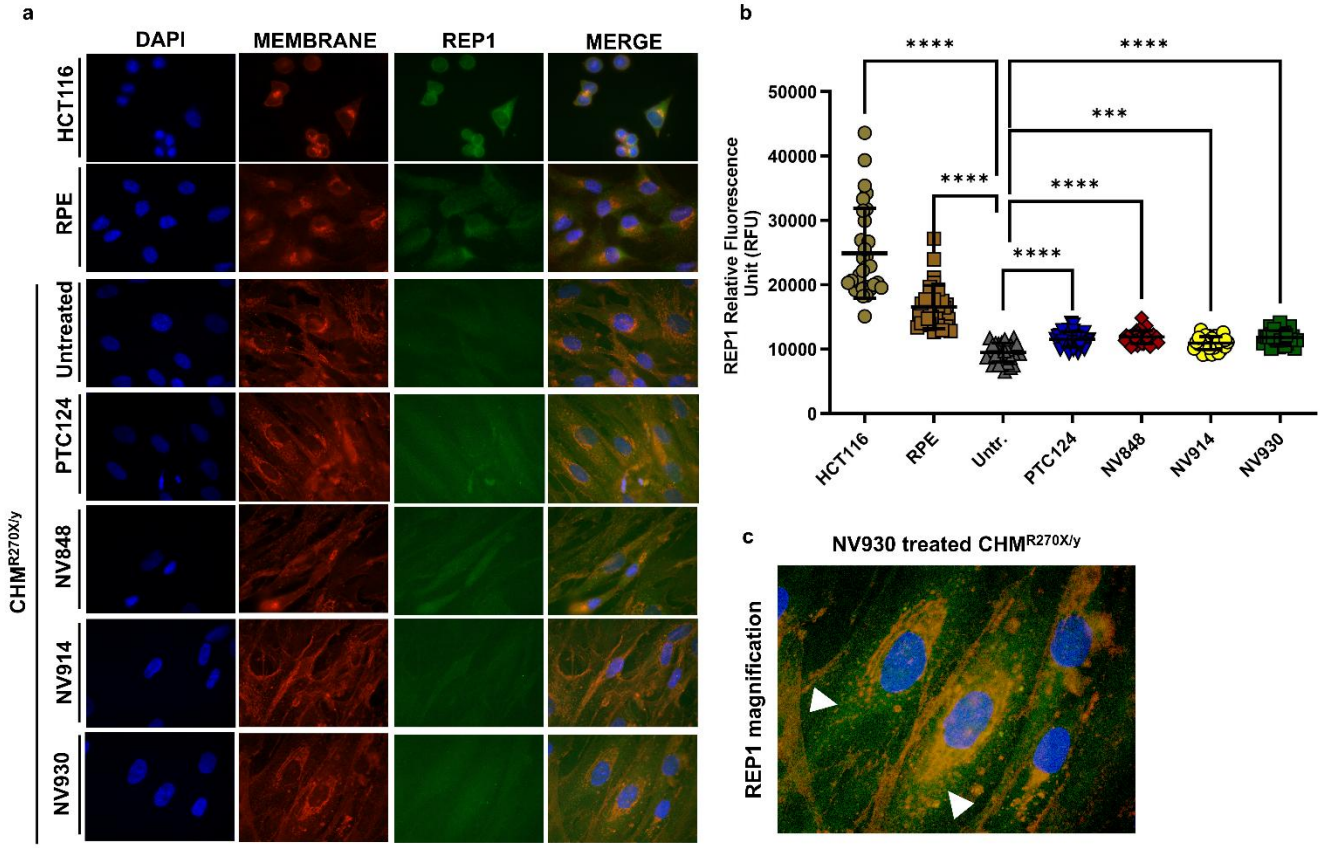


Figure 9. Immunofluorescence analyses on R270X patient-derived fibroblasts, showing the rescue of REP1 protein after 72 hours of 12 µM NV compounds treatment: ***A)*** *REP1 protein (green) was revealed by a specific primary antibody and a fluorochrome-conjugated secondary antibody (AlexaFluor-488). Nuclei (blue) were stained with DAPI (40,6-diamidino-2-phenylindole). PTC124 was used as a positive control for PTCs readthrough.* ***B)*** *Images were quantified using ImageJ, and the quantifications were analyzed using GraphPad Prism 6 software, which provided a probability value (p) of four symbols (****) for p < 0.0001;* ***C)*** *REP1 magnification image of NV930 treated CHM$^{R270X/y}$, the arrowhead shows the correct expression rescue of REP1 protein (green) inside the cells.*

Beyond protein restoration, we also assessed whether NV-mediated rescue correlates with correction of a cellular phenotype associated with REP1 deficiency. Untreated R253X fibroblasts displayed a high frequency of micronucleated cells (~23%), consistent with genomic instability linked to REP1 loss. Treatment with PTC124 or NV compounds markedly reduced micronucleation frequency, with NV848 lowering the percentage to ~10%, NV914 to ~15%, and NV930 to ~13.5% (**Figure 10).** This reduction represents a substantial normalisation of nuclear morphology compared to untreated controls. Collectively, these results demonstrate that NV compounds not only restore detectable REP1 protein in patient-derived fibroblasts but also ameliorate a cellular defect associated with REP1 deficiency. The concordance between protein rescue and phenotypic improvement strongly supports a functionally meaningful translational readthrough in primary cells.

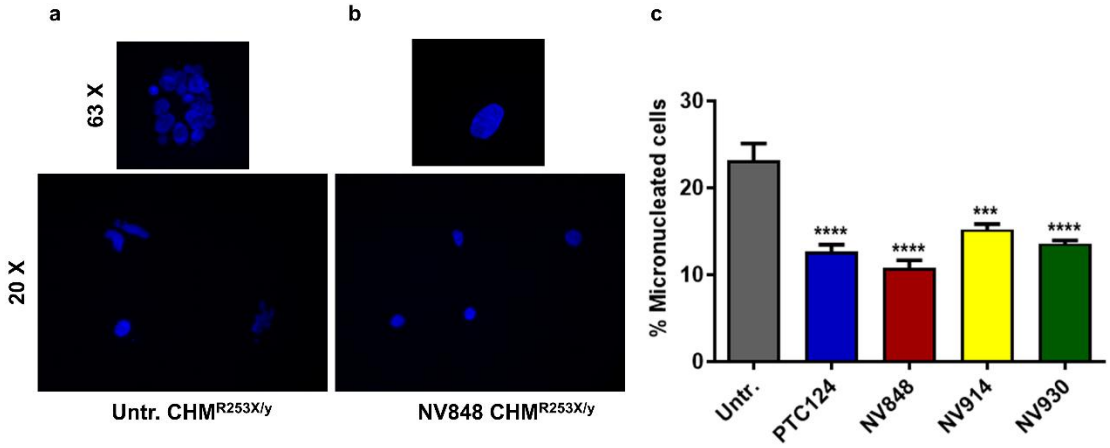


Figure 10. Micronucleated cells and their percentage in the cells: *examples of micronucleated cells present in high percentage in untreated CHM$^{R253X/y}$ (**a**) and NV848-treated CHM$^{R253X/y}$ (**b**) patient-derived fibroblasts; **c**) percentage of micronucleated cells for each condition. Data were collected using ImageJ, and all experiments were analysed using GraphPad Prism 6, which provided* a probability value (p) of three symbols (***) for $p < 0.001$ and four symbols (****) for $p < 0.0001$.

DISCUSSION

Nonsense-related diseases (NRDs) arise from nonsense variants, which account for approximately 11% of rare inherited disorders. Such variants cause premature termination codons in gene sequences, leading to the production of truncated, non-functional proteins. To date, no treatments are available for these diseases, including Cystic Fibrosis (CF), Choroideremia (CHM), and Duchenne Muscular Dystrophy (DMD). Although different approaches are now under investigation, among these, the suppression therapy approach, based on translational readthrough-inducing drugs (TRIDs), is gaining promising results. Those compounds permit the insertion of a near-cognate tRNA at the PTCs, allowing the translation of a full-length protein. Our research group has developed three compounds with readthrough activity, NV848, NV914, and NV930, that show very promising results *in vitro* and *in vivo*. In particular, all three compounds have demonstrated good readthrough activity across cell lines harbouring distinct nonsense variants [**13,19-20**].

To investigate the potential biological targets of the three NV compounds and, in addition, possible interactions with components of the translation machinery, we employed the in vitro reconstituted model system, PURE-LITE, which enables facile measurement of effects on both readthrough and termination. Our results (**Figure 3**) show that, unlike PTC124, which promotes readthrough indirectly by exclusively inhibiting eRF1/eRF3-mediated termination, NV compounds stimulate readthrough directly, at very low concentrations relative to PTC124, without affecting termination activity, suggesting a mechanism that enhances near-cognate suppressor aa-tRNA binding to the stop codon.

As a consequence of these different modes of action, NVs can act additively with PTC124 in stimulating readthrough, as shown directly for NV848 (**Figure 3-D**).

We also evaluated protein expression rescue in two Choroideremia nonsense systems to determine the NVs readthrough activity in this disease. For this purpose, we separately introduced two of the most common nonsense variants, R253X and R293X, into a plasmid, pRG213610, obtained from Origene, containing the CHM gene sequence cloned in frame with a tGFP sequence. We used vectors encoding nonsense variants to engineer H1299 cells, creating a versatile, stable model to determine the compound concentrations required to induce readthrough. Treatments were carried out at 12, 24, and 48 μM, and it was ultimately decided to proceed with 12 μM, a concentration that has previously yielded significant results in our laboratory [13,24]. Immunofluorescence analyses of the generated models revealed increased REP1 protein expression after 72 hours of chronic treatment with NV848, NV914, and NV930 (**Figures 5-6**). Next, we determined the efficacy of the three NV compounds, administered every 24 hours, in the treatment of primary human fibroblast lines derived from choroideremia patients carrying one of three nonsense variants (R253X, R270X, or S190X) in the CHM gene. The results of these new experiments indicated that the NV treatments do not appear to affect mRNA stabilisation, except for a slight effect observed in cells carrying the R253X mutation treated with NV914. Regarding CHM expression, all three fibroblast types showed similar responses to each of the three compounds, with potentially greater responsiveness in cells carrying the R253X mutation, as evidenced by immunofluorescence analysis (**Figures 7-9**). Taken together, these data suggest that NV molecules can restore REP1 protein expression in the two models by compounds that induce translational readthrough of PTCs. Furthermore, in the $CHM^{R253X/y}$ patient-derived fibroblasts, fragmented nuclei and micronuclei were clearly observed, and their frequency (23%) decreased significantly following the treatments with NV molecules (**Figure 10**), suggesting, in addition to the restoration of protein expression, a possible functional rescue of REP1 protein.

Collectively, these data demonstrate the potential of NV848, NV914, and NV930 compounds as effective agents for promoting readthrough of nonsense mutations, either alone, or in combination with nonsense suppressors acting orthogonally, across different genetic contexts, with a mechanism distinct from that of PTC124, restoring protein expression in disease-relevant cellular contexts, and may partially rescue downstream cellular phenotypes associated with REP1 loss. While further studies will be required to establish long-term functional outcomes and retinal relevance, these findings highlight NV compounds as promising candidates for nonsense suppression therapy in Choroideremia and other NRDs.

Materials and Methods

TRIDs preparation

PTC124 was either synthesised as previously described by Lentini et al. [**23**] (acid form) or provided as a gift from PTC Therapeutics as the sodium salt for PURE-LITE experiments. NV848, NV914, and NV930 were synthesised as described by Pibiri I. et al [**13**]. For all experiments, NV914 and NV930 were dissolved in DMSO and subsequently diluted in 1X PBS to 1 mM. A similar procedure was used for the cellular experiments utilising PTC124 (acid form) and NV848. PTC124 (sodium salt) and NV848 were dissolved in water for the PURE-LITE experiments.

PURE-LITE system reagents

The proteins eEF1A, eEF2, eRF1, and eRF3, and the complexes Stop-POST5, Trp-POST5, Trp-TC, Leu-TC, and RFC were prepared as previously described [**16,18**], as were the aa-tRNAs not containing a fluorescent label. Published procedures were used to prepare Atto647- Lys-$tRNA^{Lys}$ [**21**] and proflavin-labelled Trp-$tRNA^{Trp}$ [**22**]**.**

PURE-LITE system assays

Cosedimentation assays:

Cosedimentation assays, performed as described [**18**], were used to measure elongation by Trp-POST6 formation, using yeast $tRNA^{Trp}$ charged with [^{3}H]-Trp for the elongation assay measuring Trp-POST6 formation (Figure 2A) and yeast $tRNA^{Leu}$ charged with [^{3}H]-Leu for the readthrough assay measuring Stop-POST7 formation. Plate reader assays were used as described to measure Atto647-labelled pentapeptide release from the ribosome during termination [**21**] and readthrough leading to formation of ribosome-bound proflavin-labelled-stop-POST6 [**22**]. All assays were performed in Buffer 4 (40 mM Tris HCl, pH 7.5, 80 mM NH_4Cl, 5 mM $Mg(Ac)_2$,100 mM KOAc, and 3 mM β-mercaptoethanol) at 37 °C.

Cell conditions

Cell culture conditions

H1299 cells (human non-small cell lung carcinoma cell line), RPE (retinal pigment epithelium) and HCT116 (human colon rectal tumor 116) were grown in DMEM (Dulbecco's Modified Eagle Medium, GIBCO, Waltham, MA, USA) implemented with 10% FBS (fetal bovine serum, GIBCO) and 1% Penicillin and Streptomycin (Corning, USA), while patient-derived fibroblasts, purchased by Coriell Institute (New Jersey, USA), characterized separately by S190X, R253X and R270X nonsense variants were grown in MEM (Minimum Essential Medium Eagle, Thermo Fisher

Scientific, Waltham, MA, USA) implemented with 2% Ultroser G (Thermo Fisher Scientific, Waltham, MA, USA), 1% non-essential amino acids (Thermo Fisher Scientific, Waltham, MA, USA), 1% L-glutamine (Thermo Fisher Scientific, Waltham, MA, USA) and 1% Penicillin and Streptomycin (Corning, USA). Cells were cultured at 5% CO_2 and 37 °C, and media were changed every 48 hours.

Plasmid pRG213610 preparation

The pRG213610 CHM^{WT}-tGFP (**Figure S7**) plasmid was bought from Origene Technologies, Inc. (Rockville, US). It was dissolved in 100 µL of D-R-free water, briefly vortexed, and incubated at room temperature for 10 minutes. The solution was stored at -20 °C.

Site-directed mutagenesis and Colony PCR

The site-directed mutagenesis of the pRG213610 CHM^{WT}-tGFP vector with the QuickChange II kit (Stratagene, CA, USA) allowed the introduction of nonsense mutation c.757C>T (R253X) or c.877C>T (R293X) in the *CHM* coding sequence. The assay required the Pfu-Turbo DNA polymerase, plasmid template, and the following specifically designed couples of oligonucleotides, CHM-R253X For and CHM-R253X Rev, for the introduction on R253X nonsense mutation, and CHM-R293X For and CHM-R293X Rev, for the introduction of the R293X nonsense mutation (**Table S1)**. Reactions were performed as follows: 25 ng of template was incubated with 62.5 ng of each primer, 1X reaction buffer, 0.5 µl dNTP mix, and 0.5 µl Pfu Ultra from the kit. At the end of the PCR, 0.5 µl of DpnI enzyme was added, and the reactions were incubated at 37 °C for 1 h. The plasmids obtained after the mutagenesis reaction were transformed into Top10 *E. coli* competent cells, which were plated on LB agar containing ampicillin.

To select plasmid-positive colonies, colony PCR was performed with two pairs of primers, reported in **Tables S1** and **S2**, CHM For. and CHM Rev. for the R253X variant, and CHM For. and CHM-R293X Rev. for the R293X variant. The expected ~400 bp (for R293X mutation) and 1 kb (for R253X mutation) amplicons were visualised on a 1% agarose gel using SYBR Green I staining and UV exposure, and then sequenced by BMR genomics. Only one clone per mutation was used to purify mutagenized plasmid DNA using the Hi-Pure Plasmid Midi-prep Kit (Thermo Fisher Scientific, Waltham, MA, USA) according to the manufacturer's instructions. After extraction and purification, 1 µg of each DNA preparation, $pCHM^{R293X}$-tGFP and $pCHM^{R293X}$-tGFP, was sent to BMR Genomics for sequencing.

Cell Transfections

3×10^5 H1299 cells were seeded into each well of a 6-well plate (Corning, ME, USA). After 24 h, a transfection was performed. Specifically, 1 µg of pRG213610 CHM^{WT}-tGFP, 1 µg of $pCHM^{R253X}$-tGFP, or 1 µg of $pCHM^{R293X}$-tGFP was diluted separately in 200 µl of DMEM (without supplements). The transfection reagent Turbofectamine (Thermo Fisher Scientific, Waltham, MA, USA) was vortexed, and 3 µl was added to each tube containing the different plasmids. The mixtures were incubated at room temperature for 20 minutes and then dispensed into wells containing H1299 cells. After 5 h, the medium was replaced. Seventy-two hours later, selection with G418 (Geneticin) at 600 µg/mL was carried out every 72 hours for 15 days.

Cell DNA extraction

2 x 10^5 H1299, H1299 CHM^{WT}-tGFP, H1299 CHM^{R253X}-tGFP, and H1299 CHM^{R293X}-tGFP cells were seeded and, after 48 h, were detached with trypsin 0.05% (Thermo Fisher Scientific, Waltham, MA, USA), collected, and pelleted. Lastly, DNA extraction was performed using the PureLink™ Genomic DNA Mini Kit (Thermo Fisher Scientific, Waltham, MA, USA) according to the kit instructions. For each sample, DNA was quantified using a NanoDrop 2000 (Thermo Fisher Scientific, Waltham, MA, USA), and its integrity was assessed by electrophoresis on a 1% agarose gel.

PCR analysis

Genomic DNA extracted from each cell line was amplified using DreamTaq DNA Polymerase (5 U/µL; Thermo Fisher Scientific, Waltham, MA, USA) according to the manufacturer's instructions. The primers CHM For. and GFPturbo Rev., which target the plasmid region of interest, were used for the amplification (see **Table S2**) of an expected amplicon of 2049 base pairs. The PCR amplicons were visualised in a 1% agarose TAE 1X gel.

RNA extraction

RNA extraction from cells was performed using the RNeasy Mini Kit (Qiagen, Germany) following the manufacturer's instructions. In detail, fewer than 10^6 cells were lysed by brief vortexing, and an in-column DNase treatment was performed. Finally, RNA was eluted in 40 µL of DNase- and RNase-free water. This protocol was used to extract RNA from the different cell cultures, including H1299, H1299 CHM^{WT}-tGFP, H1299 CHM^{R253X}-tGFP, and H1299 CHMR293X-tGFP, Fibro CHMS190X,

and Fibro CHM^{R253X}. After the extraction for each sample, RNA was quantified using a NanoDrop 2000 (Thermo Fisher Scientific, Waltham, MA, USA), and its integrity was checked by electrophoresis on a 1% agarose gel with SYBR^{TM}-SAFE DNA Gel Stain (10,000X, Thermo Fisher Scientific, Waltham, MA, USA) staining and UV exposition.

Reverse transcription and Real Time PCR

RNAs extracted from H1299 cells (untransfected or transfected with pRG213610 CHM^{WT}-tGFP, pCHM^{R253X}-tGFP, or pCHM^{R293X}-tGFP) and from CHM$^{S190X/y}$ fibroblasts and CHM$^{R253X/y}$ fibroblasts were reverse-transcribed into cDNA using the High-Capacity cDNA Reverse Transcription Kit (Thermo Fisher Scientific, Waltham, MA, USA), according to the manufacturer's instructions. Real-time PCR was then performed using the synthesized cDNA. To evaluate TurboGFP expression, GFPturbo For. and GFPturbo Rev. primers pair were employed, while to evaluate *CHM* expression in the primary cell cultures, the primers pair CHM For. and CHM Rev. was used, GAPDH as housekeeping control, for both analyses, as detailed in **Table S2.**

For each couple of primers, the reaction mix was assembled as follows:

- PowerUp^{TM} SYBR Green Master Mix (Thermo Fisher Scientific, Waltham, USA): 5 µl;
- Primers (Forward 1 µM + Reverse 1 µM): 2 µl;
- H_2O DNase/RNase-free: 1 µl;
- cDNA: 2 µl.

The samples were loaded in triplicate with a final volume of 10 µl each. Lastly, the 96-plate was centrifuged at 2500 rpm for 5 minutes. The amplification was performed on the QuantStudio3 machine, and the results were analysed using the QuantStudio Design & Analysis Software.

Protein extraction and western blot analyses

Protein extraction from H1299 cells (untransfected or transfected with pRG213610 CHM^{WT}-tGFP, pCHM^{R253X}-tGFP, or pCHM^{R293X}-tGFP) was performed using RIPA lysis solution (Thermo Fisher Scientific, Waltham, MA, USA) and 1% protease inhibitors (Thermo Fisher Scientific, Waltham, MA, USA). Cells were lysed by brief up-and-down pipetting. Thus, the mixtures were incubated on ice at 4 °C for 1.5 h. Then, the samples were centrifuged at 12,000 rpm for 20 min at 4 °C, and the supernatants were collected and stored at -80 °C. For each sample, a quantification was performed using the Bradford colorimetric assay.

For the protein analysis, 50 µg of proteins from each sample were loaded onto a 3%-8% SDS-PAGE gel and electrophoresed at 150 V and 100 mA for 45 minutes. After that, proteins were transferred to a PVDF membrane (Thermo Fisher Scientific, Waltham, MA, USA) overnight at 4 °C, 12 V, and 50

mA. A 5% non-fat milk in TBS-TWEEN 1X solution (Thermo Fisher Scientific, Waltham, MA, USA) was used to block for 1 h at room temperature to prevent non-specific binding. The primary antibodies used were anti-REP1 (sc-23905, 1:1,000, Santa Cruz Biotechnology) and anti-β-actin antibody (A5441, 1:10,000, Sigma-Aldrich), incubating overnight at 4 °C. After three 15-minute washes with 1X PBS-Tween, the membranes were then incubated with anti-mouse horseradish peroxidase (HRP)-conjugated secondary antibody (1:5,000, Thermo Fisher Scientific). Lastly, after three 15-minute washes with 1X PBS-Tween. Protein detection was conducted by SuperSignal West Femto Maximum Sensitivity Substrate (Thermo Fisher Scientific, Waltham, MA, USA). To analyse membranes, Chemidoc XRS (BioRad) and Quantity One software (BioRad) were used. Protein bands were quantified using ImageJ software (NIH).

Immunofluorescence analysis

To assess TurboGFP protein localisation in H1299, H1299 CHM^{WT}-tGFP, H1299 CHM^{R253X}-tGFP, and H1299 CHM^{R293X}-tGFP cells, as well as REP1 protein localisation in patient-derived fibroblasts carrying the S190X, R253X, and R270X nonsense variants, 25,000 and 30,000 cells, respectively, were seeded on coverslips in 12-well plates in duplicate for each condition. Cells were subjected to chronic treatment with NV848, NV914, and NV930 for 72 h. After treatments, cells were fixed with ice-cold methanol and washed three times with 1X PBS. To visualise membranes, coverslips were incubated for 10 minutes at room temperature with anti-WGA AlexaFluor594 conjugated (1:1000). Permeabilisation was performed using 0.01% Triton X-100 for 10 min, followed by two washes with 1X PBS. Blocking was carried out with 0.1% BSA for 1 h at room temperature. Cells were then incubated overnight at 4°C with primary antibodies against TurboGFP (1:200, TA150041, Invitrogen, USA) and REP1 (1:500, Santa Cruz, USA). After three washes with 1X PBS, cells were incubated for 1 h at room temperature with an Alexa Fluor 488 conjugated anti-mouse secondary antibody (1:1000; Thermo Fisher Scientific, USA). Nuclei were counterstained with DAPI, and coverslips were mounted for imaging. Fluorescence images were acquired using a Zeiss Axioskop microscope at 63X magnification and analysed using ImageJ software (NIH). All experiments were performed in duplicate.

Statistics

Data for all experiments were analysed using GraphPad Prism 6. ANOVAs (one or two) test was performed, which provided a probability value (p) of one symbol (*) for $p<0.05$, two symbols (**) for $p < 0.01$, three symbols (***) for $p<0.001$, and four symbols (****) for $p < 0.0001$.

Author contributions

Conceptualization: L.L. B.S.C. and I.P.; **data curation:** E.V. and L.L.; **formal analysis:** E.V., R. M., S.B.; R.V., D.R.; **funding acquisition:** I.P., L.L., E.V., R.M., B.S.C.; **methodology:** E.V., R.M., S.B., S.M., and I.F.; **validation,** E.V., M.G.Z. and L.L., A.P.; **writing original draft:** E.V., L.L.; **writing, review & editing**: E.V., R.M., S.B., I.F., D.R., S.M., R.V., M.G.Z., C.R., I.P., B.S.C. and L.L. All authors have read and agreed to the published version of the manuscript.

Competing interests

The authors declare no competing interests.

Data Availability Statement

The data presented in this study are openly available at: https://iris. unipa.it/.

Acknowledgement

The results obtained in these studies were supported by grants from the Italian Ministry of University and Research (MUR), PRIN 2022 project code PRJ-0863, to I. P. and L.L. (University of Palermo), CUP B53D23008390006, and PNRR-POC project code PRJ-1839, CUP B75E24000040006, by FFR-2025 to R.M., by the Cystic Fibrosis Foundation (CFF) through the Student Traineeship Award 2023 to E.V. (award number VITALE24H0) and by research awards to B.S.C. from the CFF, COOPER23G0, and the NIH, R01GM12374.

Bibliography

1. Bidou L, Allamand V, Rousset JP, Namy O. Sense from nonsense: therapies for premature stop codon diseases. Trends Mol Med. 2012 Nov;18(11):679-88. doi: 10.1016/j.molmed.2012.09.008. Epub 2012 Oct 17. PMID: 23083810.
2. Bongiorno R, Colombo MP, Lecis D. Deciphering the nonsense-mediated mRNA decay pathway to identify cancer cell vulnerabilities for effective cancer therapy. J Exp Clin Cancer Res. 2021 Dec 1;40(1):376. doi: 10.1186/s13046-021-02192-2. PMID: 34852841; PMCID: PMC8638473.
3. Goetz LH, Schork NJ. Personalised medicine: motivation, challenges, and progress. Fertil Steril. 2018 Jun;109(6):952-963. doi: 10.1016/j.fertnstert.2018.05.006. PMID: 29935653; PMCID: PMC6366451.
4. Vitale E, Ricci D, Corrao F, Fiduccia I, Cruciata I, Carollo PS, Branchini A, Lentini L, Pibiri I. Nonsense Mutations in Rare and Ultra-Rare Human Disorders: An Overview. IUBMB Life. 2025 Jun;77(6):e70031. doi: 10.1002/iub.70031. PMID: 40474765; PMCID: PMC12142302.
5. Ricci D, Cruciata I, Fiduccia I, Vitale E, Corrao F, Branchini A, Carollo PS, Pibiri I, Lentini L. Advancing Therapeutic Strategies for Nonsense-Related Diseases: From Small Molecules to Nucleic Acid-Based Innovations. IUBMB Life. 2025 May;77(5):e70027. doi: 10.1002/iub.70027. PMID: 40420818; PMCID: PMC12107293.
6. Dabrowski M, Bukowy-Bieryllo Z, Zietkiewicz E. Advances in therapeutic use of a drug-stimulated translational readthrough of premature termination codons. Mol Med. 2018 May 29;24(1):25. doi: 10.1186/s10020-018-0024-7. PMID: 30134808; PMCID: PMC6016875.
7. Campofelice A, Lentini L, Di Leonardo A, Melfi R, Tutone M, Pace A, Pibiri I. Strategies against Nonsense: Oxadiazoles as Translational Readthrough-Inducing Drugs (TRIDs). Int J Mol Sci. 2019 Jul 6;20(13):3329. doi: 10.3390/ijms20133329. PMID: 31284579; PMCID: PMC6651739.
8. Li S, Li J, Shi W, Nie Z, Zhang S, Ma F, Hu J, Chen J, Li P, Xie X. Pharmaceuticals Promoting Premature Termination Codon Readthrough: Progress in Development. Biomolecules. 2023 Jun 14;13(6):988. doi: 10.3390/biom13060988. PMID: 37371567; PMCID: PMC10296333.
9. Welch EM, Barton ER, Zhuo J, Tomizawa Y, Friesen WJ, Trifillis P, Paushkin S, Patel M, Trotta CR, Hwang S, Wilde RG, Karp G, Takasugi J, Chen G, Jones S, Ren H, Moon YC, Corson D, Turpoff AA, Campbell JA, Conn MM, Khan A, Almstead NG, Hedrick J, Mollin A, Risher N, Weetall M, Yeh S, Branstrom AA, Colacino JM, Babiak J, Ju WD, Hirawat S, Northcutt VJ, Miller LL, Spatrick P, He F, Kawana M, Feng H, Jacobson A, Peltz SW, Sweeney HL. PTC124 targets genetic disorders caused by nonsense mutations. Nature. 2007 May 3;447(7140):87-91. doi: 10.1038/nature05756. Epub 2007 Apr 22. PMID: 17450125.
10. Michorowska S. Ataluren-Promising Therapeutic Premature Termination Codon Readthrough Frontrunner. Pharmaceuticals (Basel). 2021 Aug 9;14(8):785. doi: 10.3390/ph14080785. PMID: 34451881; PMCID: PMC8398184.
11. McDonald CM, Campbell C, Torricelli RE, Finkel RS, Flanigan KM, Goemans N, Heydemann P, Kaminska A, Kirschner J, Muntoni F, Osorio AN, Schara U, Sejersen T, Shieh PB, Sweeney HL,

Topaloglu H, Tulinius M, Vilchez JJ, Voit T, Wong B, Elfring G, Kroger H, Luo X, McIntosh J, Ong T, Riebling P, Souza M, Spiegel RJ, Peltz SW, Mercuri E; Clinical Evaluator Training Group; ACT DMD Study Group. Ataluren in patients with nonsense mutation Duchenne muscular dystrophy (ACT DMD): a multicentre, randomised, double-blind, placebo-controlled, phase 3 trial. Lancet. 2017 Sep 23;390(10101):1489-1498. doi: 10.1016/S0140-6736(17)31611-2. Epub 2017 Jul 17. PMID: 28728956.

12. Duan D, Goemans N, Takeda S, Mercuri E, Aartsma-Rus A. Duchenne muscular dystrophy. Nat Rev Dis Primers. 2021 Feb 18;7(1):13. doi: 10.1038/s41572-021-00248-3. PMID: 33602943; PMCID: PMC10557455.
13. Pibiri I, Melfi R, Tutone M, Di Leonardo A, Pace A, Lentini L. Targeting Nonsense: Optimization of 1,2,4-Oxadiazole TRIDs to Rescue CFTR Expression and Functionality in Cystic Fibrosis Cell Model Systems. Int J Mol Sci. 2020 Sep 3;21(17):6420. doi: 10.3390/ijms21176420. PMID: 32899265; PMCID: PMC7504161.
14. Corrao F, Zizzo MG, Tutone M, Melfi R, Fiduccia I, Carollo PS, Leonardo AD, Caldara G, Perriera R, Pace A, Belmonte B, Sammataro S, Pibiri I, Lentini L. Nonsense codons suppression. An acute toxicity study of three optimized TRIDs in a murine model, safety and tolerability evaluation. Biomed Pharmacother. 2022 Dec;156:113886. doi: 10.1016/j.biopha.2022.113886. Epub 2022 Oct 18. PMID: 36265311.
15. Perriera R, Vitale E, Pibiri I, Carollo PS, Ricci D, Corrao F, Fiduccia I, Melfi R, Zizzo MG, Tutone M, Pace A, Lentini L. Readthrough Approach Using NV Translational Readthrough-Inducing Drugs (TRIDs): A Study of the Possible Off-Target Effects on Natural Termination Codons (NTCs) on TP53 and Housekeeping Gene Expression. Int J Mol Sci. 2023 Oct 11;24(20):15084. doi: 10.3390/ijms242015084. PMID: 37894764; PMCID: PMC10606485.
16. Huang S, Bhattacharya A, Ghelfi MD, Li H, Fritsch C, Chenoweth DM, Goldman YE, Cooperman BS. Ataluren binds to multiple protein synthesis apparatus sites and competitively inhibits release factor-dependent termination. Nat Commun. 2022 May 6;13(1):2413. doi: 10.1038/s41467-022-30080-6. PMID: 35523781; PMCID: PMC9076611.
17. Ng MY, Zhang H, Weil A, Singh V, Jamiolkowski R, Baradaran-Heravi A, Roberge M, Jacobson A, Friesen W, Welch E, Goldman YE, Cooperman BS. New *in Vitro* Assay Measuring Direct Interaction of Nonsense Suppressors with the Eukaryotic Protein Synthesis Machinery. ACS Med Chem Lett. 2018 Nov 21;9(12):1285-1291. doi: 10.1021/acsmedchemlett.8b00472. PMID: 30613341; PMCID: PMC6295867.
18. Ng MY, Li H, Ghelfi MD, Goldman YE, Cooperman BS. Ataluren and aminoglycosides stimulate the read-through of nonsense codons by orthogonal mechanisms. Proc Natl Acad Sci U S A. 2021 Jan 12;118(2):e2020599118. doi: 10.1073/pnas.2020599118. PMID: 33414181; PMCID: PMC7812769.
19. Bezzerri V, Lentini L, Api M, Busilacchi EM, Cavalieri V, Pomilio A, Diomede F, Pegoraro A, Cesaro S, Poloni A, Pace A, Trubiani O, Lippi G, Pibiri I, Cipolli M. Novel Translational Read-through-

Inducing Drugs as a Therapeutic Option for Shwachman-Diamond Syndrome. Biomedicines. 2022 Apr 12;10(4):886. doi: 10.3390/biomedicines10040886. PMID: 35453634; PMCID: PMC9024944.

20. Fiduccia I, Corrao F, Zizzo MG, Perriera R, Genovese F, Vitale E, Ricci D, Melfi R, Tutone M, Pace A, Lentini L, Pibiri I. Promoting readthrough of nonsense mutations in CF mouse model: Biodistribution and efficacy of NV848 in rescuing CFTR protein expression. Mol Ther. 2024 Dec 4;32(12):4514-4523. doi: 10.1016/j.ymthe.2024.10.028. Epub 2024 Oct 28. PMID: 39473179; PMCID: PMC11638873.
21. Ghelfi MD, Bhat SY, Li H, Cooperman BS. A High-Throughput Assay for In Vitro Determination of Release Factor-Dependent Peptide Release from a Pretermination Complex by Fluorescence Anisotropy-Application to Nonsense Suppressor Screening and Mechanistic Studies. Biomolecules. 2023 Jan 27;13(2):242. doi: 10.3390/biom13020242. PMID: 36830611; PMCID: PMC9953321.
22. Bhat SY, Bhattacharya A, Li H, Cui X, Lueck JD, Goldman YE, Cooperman BS. Mechanism-based approach in designing patient-specific combination therapies for nonsense mutation diseases. Nucleic Acids Res. 2025 Mar 20;53(6):gkaf216. doi: 10.1093/nar/gkaf216. PMID: 40156864; PMCID: PMC11954524.
23. Lentini L, Melfi R, Di Leonardo A, Spinello A, Barone G, Pace A, Palumbo Piccionello A, Pibiri I. Toward a rationale for the PTC124 (Ataluren) promoted readthrough of premature stop codons: a computational approach and GFP-reporter cell-based assay. Mol Pharm. 2014 Mar 3;11(3):653-64. doi: 10.1021/mp400230s. Epub 2014 Feb 7. PMID: 24483936; PMCID: PMC4167060.
24. Fiduccia I, Vitale E, Varrica R, Ricci D, Marino S, Zito A, Pace A, Colige A, Moutschen M, Borutzki Y, Bileck A, Meier-Menches SM, Lentini L, Pibiri I. Beyond the stop: Oxadiazole TRIDs restore LRBA protein expression in nonsense-driven primary immunodeficiency. Mol Ther Nucleic Acids. 2025 Dec 18;37(1):102808. doi: 10.1016/j.omtn.2025.102808. PMID: 41541268; PMCID: PMC12803801.

Supplementary informations

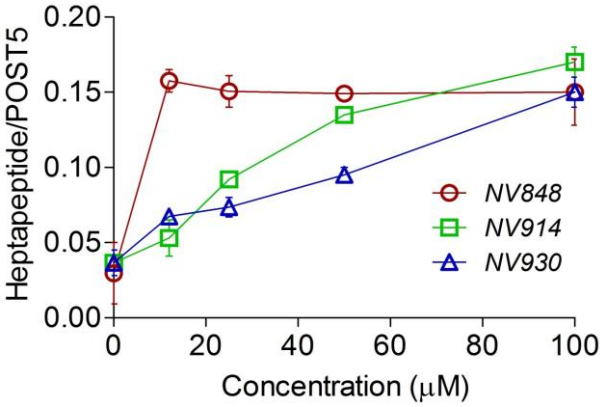


Figure S1. Readthrough dependence on NV compound concentrations. *The readthrough activity was measured using the Stop-POST 7 heptapeptide co-sedimentation assay, for up to 100 µM of each compound. Other concentrations: Stop-POST5 (0.05 µM), eRF1 (0.05 µM), eRF3 (0.1 µM),Trp-TC (0.25 µM), [^{3}H-Leu]-TC (0.25µM), eEF2 (1µM), GTP (1 mM).*

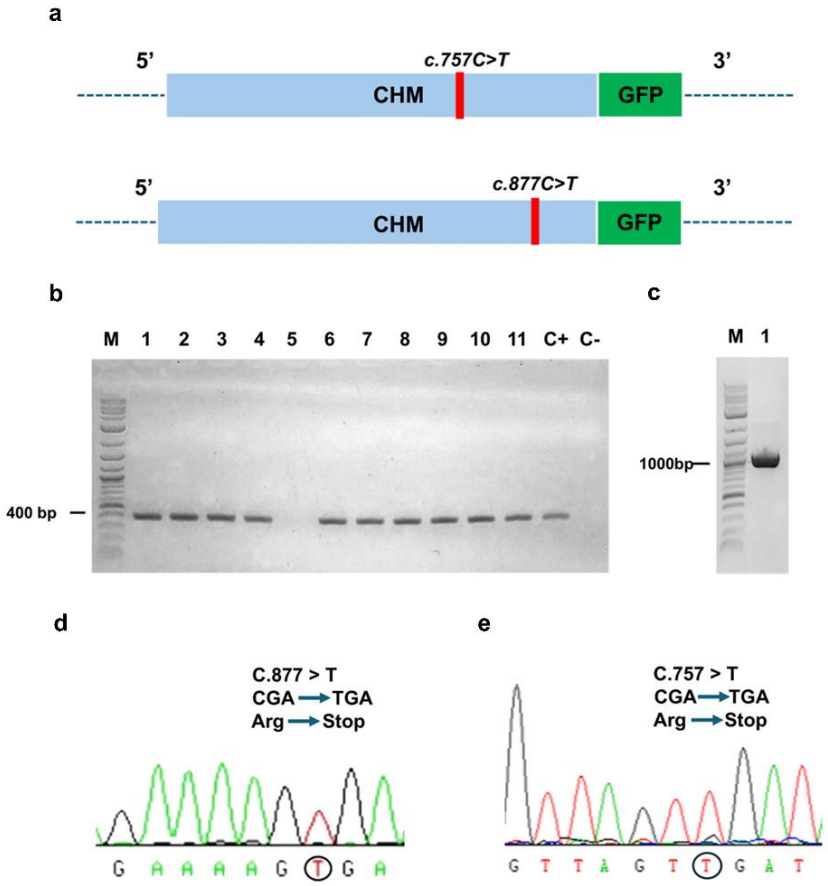


Figure S2. R253X and R293X nonsense variants insertion and validation by colony PCR and Sanger Sequencing: a) *schematic representation of the nonsense mutations introduced into the CHM cDNA sequence in the pRG213610 CHM^{WT}-tGFP plasmid; Colony PCR assay to evaluate the*

*presence of the pRG213610 CHM^{R293X}-tGFP (**b**) or pRG213610 CHM^{R253X}-tGFP (**c**) in bacterial cells. Each lane represents a clone; M: 2-log ladder; C+: positive control (pRG213610 CHM^{WT} tGFP); C-: No Template control; Sanger sequencing chromatograms showing the substitutions c.877C>T (R293X) (**d**) or c.757C>T (R253X) (**e**) in CHM cDNA.*

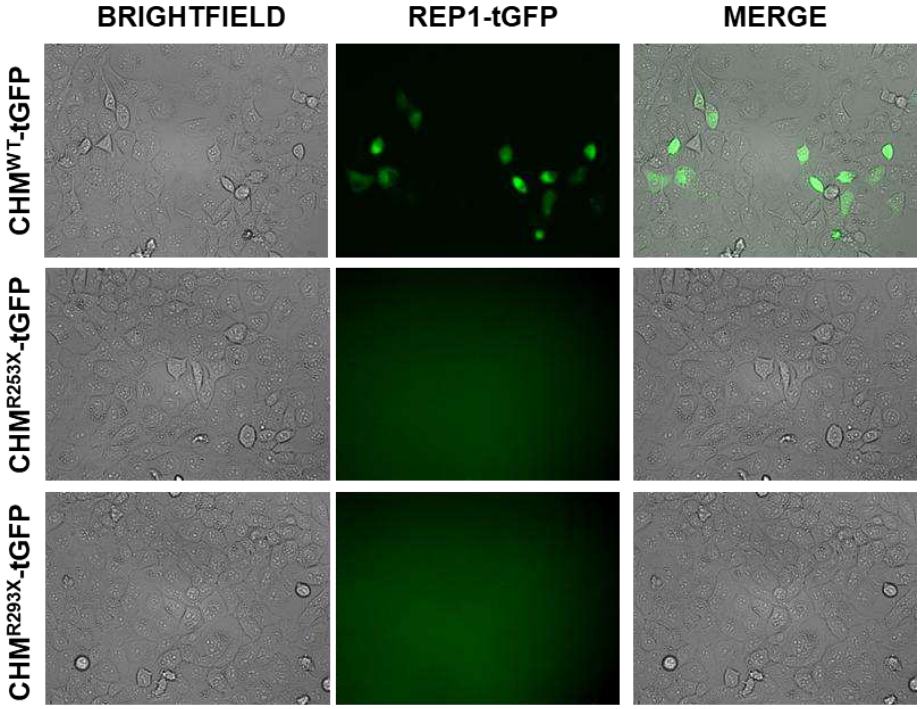


Figure S3. tGFP fluorescence emission after 24 hours post-transfection: *the panel shows tGFP fluorescence 24 hours post-transfection in H1299 cells transfected with pCHM^{WT}-tGFP, while the H1299 cells transfected with mutagenized plasmids do not show tGFP expression.*

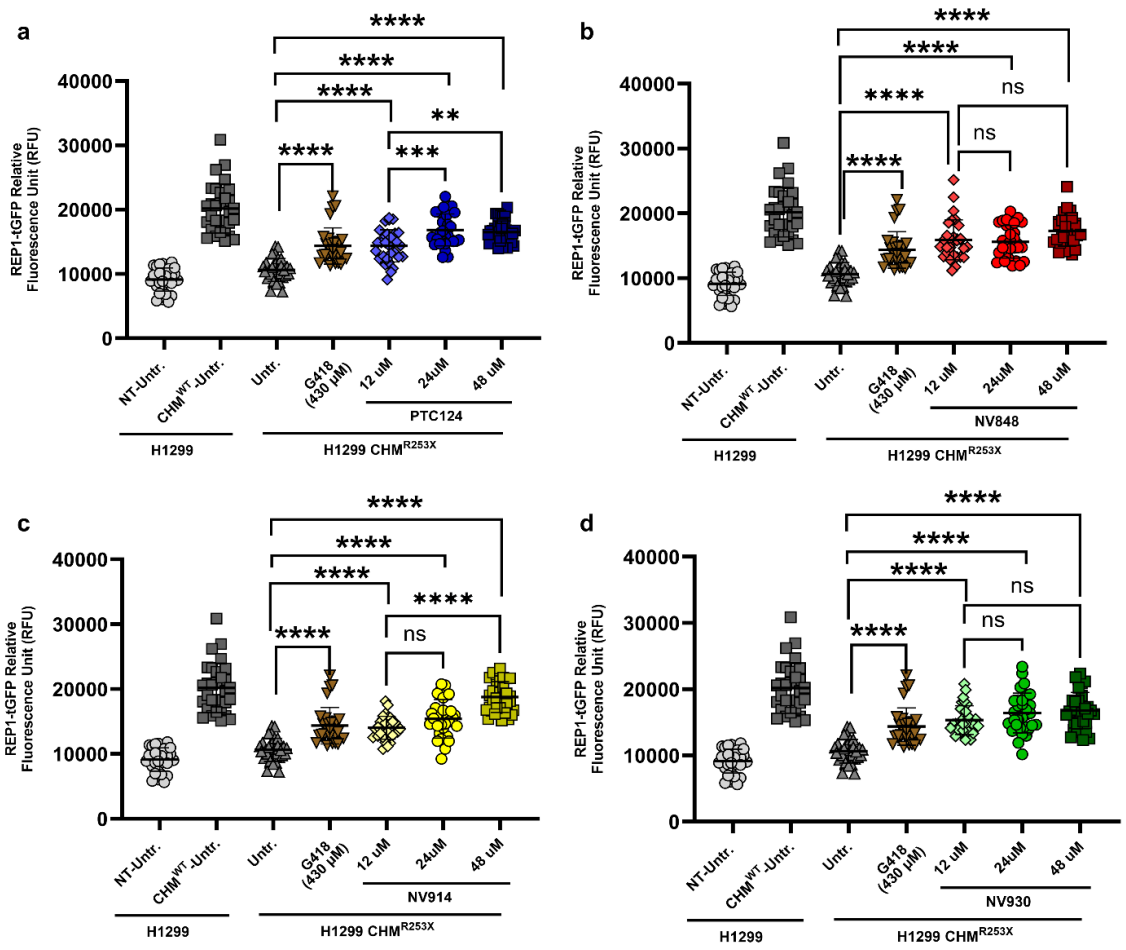


Figure S4. Immunofluorescence analysis: *Treatments were performed with PTC124 (**a**), NV848 (**b**), NV914 (**c**), and NV930 (**d**) at concentrations of 12, 24, and 48 µM in a stable H1299 CHM^{R253X}-tGFP cell line. Untransfected H1299 cells and untreated stable cell lines served as negative controls, whereas G418 at 430 µM served as the positive control. Data for all experiments were analysed using GraphPad Prism 6, which provided a* probability value (p) of two symbols (**) for $p < 0.01$, three symbols (***) for $p<0.001$, and four symbols (****) for $p < 0.0001$.

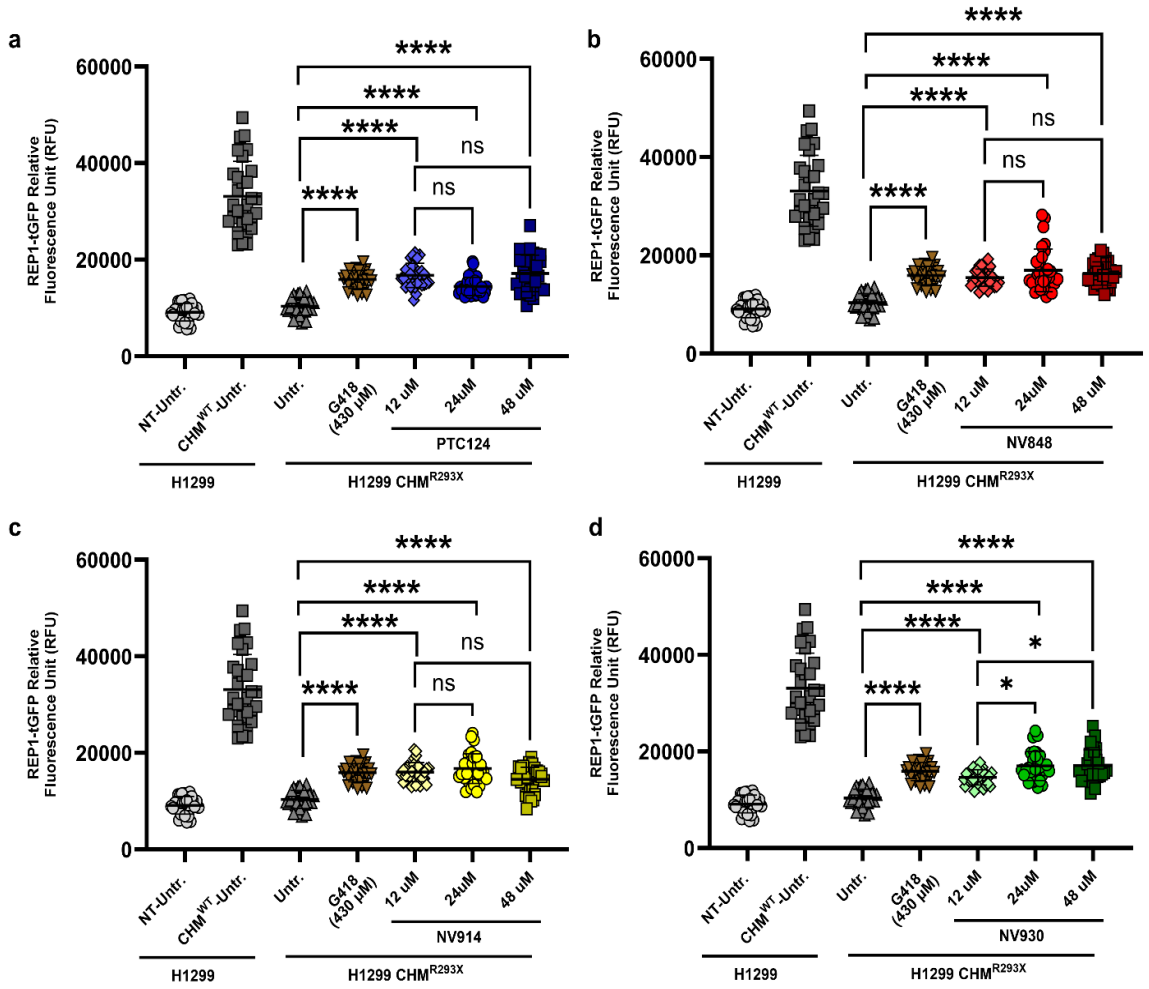


Figure S5. Immunofluorescence analysis: *Treatments were performed with PTC124 (**a**), NV848 (**b**), NV914 (**c**), and NV930 (**d**) at concentrations of 12, 24, and 48 µM in a stable H1299 CHM^{R293X}-tGFP cell line. Untransfected H1299 cells and untreated stable cell lines served as negative controls, whereas G418 at 430 µM served as the positive control. Data for all experiments were analysed using GraphPad Prism 6, which provided a* probability value (p) of one symbol (*) for $p < 0.05$, two symbols (**) for $p < 0.01$, three symbols (***) for $p<0.001$, four symbols (****) for $p < 0.0001$.

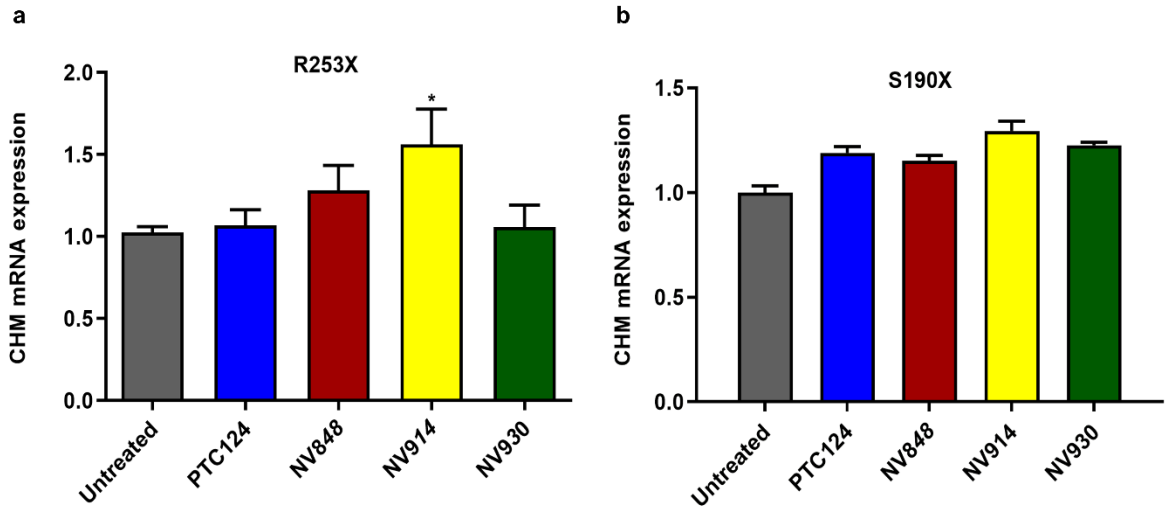


Figure S6. CHM mRNA expression in* CHM$^{R253X/y}$ and CHM$^{S190X/y}$ *fibroblasts following 72 hours of chronic treatment: a) *an increase in CHM$^{R253X/y}$ transcripts patient patient-derived fibroblast is revealed after NV914 treatment;* ***b)*** *no increase in CHM $^{S190X/y}$ transcripts patient patient-derived fibroblast is shown. Each experiment was analyzed using GraphPad Prism 6, which provided a* probability value (p) of one symbol (*) for $p < 0.05$.

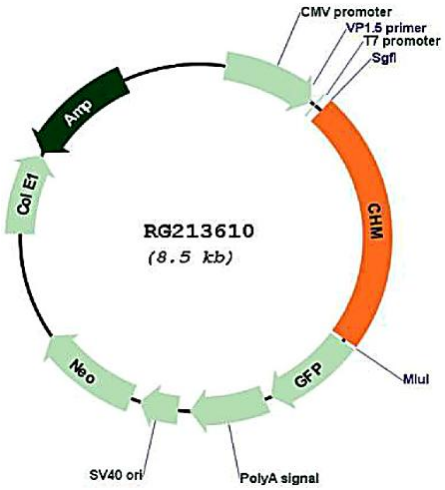


Figure S7. pRG213610 plasmid map: *The vector contains the CHM sequence with an in-frame sequence for turbo GFP, an Amp cassette for the selection in bacterial cells, and a Neo cassette for selection in eukaryotic cells.*

Primer	Sequence 5’ - 3’
CHM-R253X For.	**5'**-ATTGATCTTCTAATCAAATCTAATGTTAGT**T**GATATGCAGAG TTTAAAAATATTACCA-**3’**
CHM-R253X Rev.	**5'**-TGGTAATATTTTTAAACTCTGCATATC**A**ACTAACATTAGATT TGATTAGAAGATCAAT-**3’**
CHM-R293X For.	**5'**-GCAAACAACTTACTATGGTAGAAAAG**T**GAATGCTAATGAAA TTTCTTACATTT-**3'**
CHM-R293X Rev.	**5'**-AAATGTAAGAAATTTCATTAGCATTC**A**CTTTTCTACCATAGT AAGTTGTTTGC-**3′**

Table S1. Primer sequences for site-directed mutagenesis: *primer sequences used for the introduction of the nonsense variants in the pRG213610 CHM^{WT}-tGFP.*

Primer	Sequence 5’ - 3’
CHM For.	**5’**-GATCCAGAGAATGCGCTAG-**3’**
CHM Rev.	**5’**-AATGACCCGAACAGCAAAAGTTC-**3’**
GAPDH For.	**5’**-CTCATGACCACAGTCCATGCC-**3’**
GAPDH Rev.	**5’**-GCCATCCACAGTCTTCTGGGT-**3’**
GFPturbo For.	**5’**-AGGACAGCGTGATCTTCACC-**3’**
GFPturbo Rev.	**5’**-CTTGAAGTGCATGTGGCTGT-**3’**

Table S2. Primer sequences involved in Real-time qPCR and endpoint PCR.